ARTICLES

Interhemispheric Atlantic seesaw response during the last deglaciation

Stephen Barker[1], Paula Diz[1]†, Maryline J. Vautravers[2], Jennifer Pike[1], Gregor Knorr[1]†, Ian R. Hall[1] & Wallace S. Broecker[3]

The asynchronous relationship between millennial-scale temperature changes over Greenland and Antarctica during the last glacial period has led to the notion of a bipolar seesaw which acts to redistribute heat depending on the state of meridional overturning circulation within the Atlantic Ocean. Here we present new records from the South Atlantic that show rapid changes during the last deglaciation that were instantaneous (within dating uncertainty) and of opposite sign to those observed in the North Atlantic. Our results demonstrate a direct link between the abrupt changes associated with variations in the Atlantic meridional overturning circulation and the more gradual adjustments characteristic of the Southern Ocean. These results emphasize the importance of the Southern Ocean for the development and transmission of millennial-scale climate variability and highlight its role in deglacial climate change and the associated rise in atmospheric carbon dioxide.

The last glacial and deglacial periods were characterized by millennial-scale shifts in global climate. Records from Greenland ice cores[1] and North Atlantic sediments[2,3] suggest that high latitudes in the Northern Hemisphere were repeatedly subjected to large and abrupt fluctuations in temperature, commonly referred to as Dansgaard–Oeschger oscillations. In contrast to the abrupt changes observed in the north, temperature fluctuations over Antarctica were more gradual (warming and cooling over hundreds to thousands of years) and approximately out of phase with their northern counterparts[4]. Recent ice-core evidence from the Atlantic sector of Antarctica reveals a direct relationship between the extent of warming across Antarctica and the duration of cold, stadial conditions over Greenland[5]. The contrasting behaviour of temperature variations over Greenland and the North Atlantic as compared with Southern Hemisphere records has led to the notion of a bipolar seesaw, whereby changes in the strength of the Atlantic's conveyor circulation or, more precisely, the Atlantic meridional overturning circulation (AMOC) affect the distribution of heat between the South Atlantic and the North Atlantic and more widely[6,7]. Modelling results[8] suggest that a reduction in the strength of the AMOC (for example as may be caused by an input of fresh water to the North Atlantic) would give rise to an immediate decrease in northward heat transport. As a result, surface air temperatures over the North Atlantic would cool and those over the South Atlantic would warm. The transmission of these anomalies between the North Atlantic and the South Atlantic may take on the order of a few decades[8–10].

Although the bipolar seesaw can explain the antiphase relationship between Greenland and Antarctic temperature fluctuations through changes in the strength of the AMOC, it does not immediately account for the contrasting nature of the two signals. The simplest mechanism for transposing between the abrupt nature of Dansgaard–Oeschger oscillations and the more gradual temperature fluctuations observed over Antarctica involves the heat capacity of the Southern Ocean. This conceptual model (the ''thermal bipolar seesaw''[11]) implies that temperature fluctuations in the South Atlantic should display an inverse form of the northern temperature signal whereas those further south should be more gradual in nature[11]. However, so far all marine temperature reconstructions from the Southern Hemisphere (outside the tropics[12]) tend to resemble those from Antarctica (that is, with more gradual warming and cooling phases), and although a recent reconstruction from the southeast Pacific indicates a slightly more rapid response[13], a truly abrupt counterpart to the Northern Hemisphere variations has not yet been observed.

The last deglacial period (Termination I) witnessed several abrupt climatic shifts. During early Termination I (~18–14.6 kyr ago), temperature records from Greenland and the North Atlantic reveal a cold interval (Heinrich stadial 1 (HS1)) during which the massive ice-rafting episode known as Heinrich event 1 occurred (we use the term 'Heinrich stadial' to denote a stadial which contains a Heinrich event—a Heinrich stadial is not equivalent to a Heinrich event). This was followed by an abrupt and significant warming into the Bølling–Allerød warm interval before a rapid return to near-glacial conditions during the Younger Dryas event (~12.8–11.5 kyr ago). The final transition to Holocene warmth was completed by about 10 kyr ago. So far, changes observed in the Southern Hemisphere across Termination I were typically more gradual. Warming occurred during the period of severe North Atlantic cold (HS1) and was followed by a pause in warming (or a slight cooling), known as the Antarctic Cold Reversal, during the Bølling–Allerød interval. Completion of deglacial warming over Antarctica was accomplished during the Younger Dryas interval. A recent reconstruction of AMOC variability through Termination I[14] suggests that overturning within the Atlantic basin was severely affected during the cold episodes of Northern Hemisphere deglaciation. During HS1, cold conditions across the North Atlantic and warming over Antarctica were associated with a strong reduction in overturning strength[14]. A similar but less pronounced weakening occurred during the Younger Dryas. The slowdown of the AMOC and the coincident rise in Antarctic temperature and atmospheric CO_2 during the extreme (northern) cold of HS1 has been highlighted as a possible driving factor for the last termination[15]. This suggests that the bipolar seesaw

[1]School of Earth and Ocean Sciences, Cardiff University, Cardiff CF10 3YE, UK. [2]British Antarctic Survey, Cambridge CB3 0ET, UK. [3]Lamont-Doherty Earth Observatory of Columbia University, Palisades, New York 10964-8000, USA. †Present addresses: Laboratoire des Bio-Indicateurs Actuels et Fossiles, Angers University, 49045 Angers Cedex 01, France (P.D.); Alfred Wegener Institute, 27570 Bremerhaven, Germany (G.K.).

is a key component not only for millennial-scale climate variability but also for changes on glacial–interglacial timescales. As such, increasing our understanding of the physical links between north and south at millennial timescales is critical for understanding the potential role of such variability as a feedback on global climate change[16].

Deglacial changes in the South Atlantic

Here we present continuous and high-resolution multi-proxy records spanning the late glacial and deglacial period from a marine sediment core (TNO57-21). Located in the southeast Atlantic Ocean (41.1° S, 7.8° E, 4,981-m water depth), at the northern margin of the modern Antarctic Circumpolar Current (ACC), the core is ideally positioned to capture an inverse form of the North Atlantic signal as predicted by the seesaw model (Fig. 1). Previous studies have illustrated the high quality of this core as a paleoceanographic archive (see, for example, refs 17, 18). We have measured 19 monospecific planktonic radiocarbon ages to provide an independent and absolute age model for the core (Supplementary Information). To investigate changes in surface ocean temperatures, we use a combination of planktonic foraminiferal assemblage counts and Mg/Ca ratios measured on the planktonic foraminifera *Globigerina bulloides*. We also analysed the benthic foraminiferal fauna and diatoms to investigate changes in the nature of productivity in the surface ocean.

Figure 2 shows our surface ocean records from TNO57-21 for the late glacial and deglacial period, plotted with temperature records from Greenland[1], Antarctica[5,19], the North Atlantic[2] and the southeast Pacific[13] along with the $^{231}Pa/^{230}Th$-based AMOC reconstruction of ref. 14. The relative abundance of polar planktonic foraminiferal species (*Neogloboquadrina pachyderma* (sinistral) and

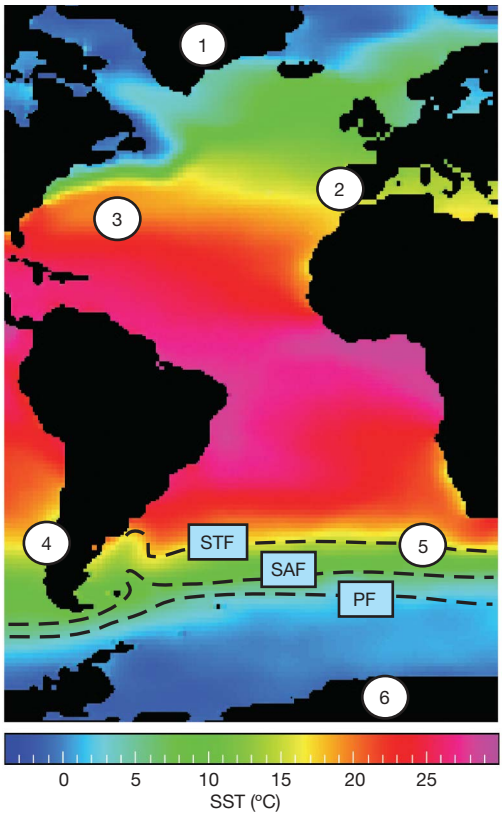

Figure 1 | Map showing sea surface temperature (SST)[50] and the positions of records shown in Fig. 2. Position 1, Greenland ice core GISP2 (ref. 1); 2, marine core SU8118 (ref. 2); 3, marine core OCE326-GGC5 (ref. 14); 4, marine core ODP 1233 (ref. 13); 5, marine core TNO57-21 (this study); 6, Antarctic ice core EDML (EPICA Dronning Maud Land)[5]. Dashed lines are approximate positions of the major oceanic fronts of the ACC: STF, Subtropical Front; SAF, Sub-Antarctic Front; PF, Polar Front.

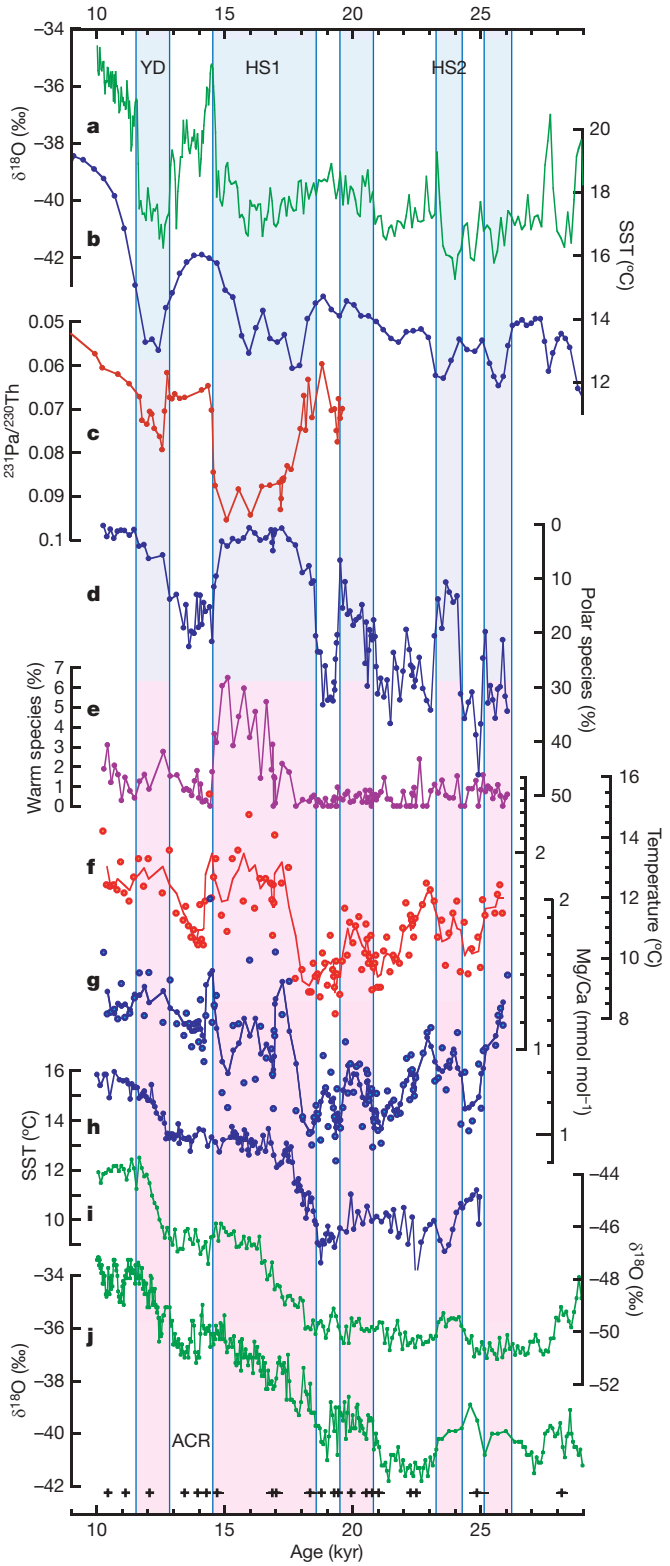

Figure 2 | Deglacial records from TNO57-21 plus other proxy records for temperature and circulation within the Atlantic Ocean. a, Greenland temperature (GISP2 ice core)[1]; **b**, North Atlantic SST (core SU8118)[2]; **c**, AMOC strength derived from sedimentary $^{231}Pa/^{230}Th$ ratio[14] (higher values indicate a reduced AMOC); **d**, polar foraminiferal species in TNO57-21; **e**, warm species; **f**, Mg/Ca ratio (and calculated calcification temperature) in *G. bulloides*, adjusted to account for dissolution; **g**, measured Mg/Ca ratio in *G. bulloides* (solid lines in **f** and **g** are three-point running means); **h**, southeast Pacific SST[13]; **i**, **j**, Antarctic temperature (EDML[5] and Byrd[4,19] ice cores, respectively). Black symbols at the bottom indicate dating control points (calendar age uncertainty is 1σ; Supplementary Table 1). Shaded boxes represent periods of warmth or warming in the south according to our records.

Turborotalita quinqueloba; Fig. 2d) in TNO57-21 reveals large (>10%) and abrupt (~100-yr) changes throughout the interval. Moreover, within the uncertainties of our dating control (Supplementary Information) the abrupt shifts in assemblage are simultaneous with the abrupt transitions observed in the north. For example, the reduction in the AMOC (Fig. 2c) and associated cooling during HS1 (Fig. 2a, b) is matched by a sharp decline of polar species (a warming) in TNO57-21. A similar correspondence is observed during HS2 and the Younger Dryas. Conversely, warming events in the north (such as the Bølling–Allerød warming ~14.6 kyr ago and the Dansgaard–Oeschger event 2 ~23 kyr ago) are aligned with cooling in the south.

The abrupt nature of changes observed in TNO57-21 may be contrasted with the more gradual changes displayed in the temperature records from Antarctica (Fig. 2i, j) and the southeast Pacific (Fig. 2h). Periods of warming in the Antarctic record (for example during the Younger Dryas, HS1 and HS2) tend to begin in parallel with an abrupt decrease in polar species recorded in TNO57-21 and to end when polar species increase again (except for the end of the Younger Dryas, by which time mean conditions were presumably too warm for these species). Thus, the Antarctic signal resembles a damped, or integrated, form of the South Atlantic record. Our record also shows warming episodes ~21 and ~26 kyr ago. Both of these are aligned with warm intervals in the Byrd ice-core record from Antarctica[4] (Fig. 2j), and the earlier event apparently corresponds to a cool episode in the North Atlantic[2] (Fig. 2b). The warming ~21 kyr ago represents the end of significant ice-rafted debris at the site of TNO57-21[18] (Supplementary Fig. 8) and is apparent in records from both hemispheres (Fig. 2), perhaps representing an early phase of global deglacial warming.

The modern distribution of planktonic foraminiferal species in the South Atlantic and the adjacent sector of the Southern Ocean is dominated by the strong temperature gradients associated with the frontal systems of the ACC[20]. For example, polar species dominate the modern assemblage south of the present-day SAF but are virtually absent north of the STF. This change occurs within about 5° of latitude as a result of the SST gradient of >7 °C between the SAF and the STF (Fig. 1). Core TNO57-21 lies roughly beneath the STF in its modern position. As such, a relatively modest latitudinal shift or modulation of the frontal system (a few degrees) could cause a large (>20%) change in the abundance of polar species. We infer that the abrupt transitions in polar species observed in TNO57-21 during the deglacial period (Fig. 2d) represent shifts in the northern fronts associated with the ACC. Our results suggest a direct link between abrupt changes at high northern latitudes and similarly abrupt variations in the geometry of the ACC.

In the early part of the record, the abrupt decreases in polar species (notably HS2) were mainly accommodated by increases in the subpolar species, *N. pachyderma* (dextral). During deglaciation transitional species (for example *G. bulloides* and *Globorotalia inflata*) became more common and replaced both polar and subpolar species during the latest warming event. The appearance of warm-water species (*Globorotalia truncatulinoides* (dextral), *Globigerinoides ruber*, *Globorotalia hirsuta* and *Orbulina universa*; Fig. 2e) during HS1 (just before the Antarctic Cold Reversal) indicates that this was the warmest interval of the entire deglacial period, including the earliest Holocene, and highlights the anomalous conditions across the Atlantic during this time (in the modern South Atlantic, these species are only abundant well to the north of the STF[20]). It should be noted that we see no significant fluctuations in the contribution of faunas associated with the leakage of warm Indian Ocean water around the southern tip of Africa[21]. The 'Agulhas leakage' fauna in TNO57-21 show a relatively monotonic decrease throughout the interval, driven primarily by changes in the abundance of a single species, *Globigerinita glutinata*. We suggest that our record reflects a general warming of the South Atlantic during HS1 (as suggested by previous studies[22–24]) that may include the effect of increased Agulhas leakage during this time[21]. Furthermore, a reconstruction from 20° S in the western South Atlantic also suggests that sea surface temperatures in this region reached values comparable to, if not higher than, modern conditions during HS1[22].

Ambient temperature response

The more gradual appearance of warm-water foraminiferal species during HS1 (in contrast to the rapid fluctuations implied by the polar fauna) is reminiscent of Antarctic warming, that is, is influenced by the thermal inertia of a large water mass, and possibly reflects an increase in ambient temperatures in the South Atlantic region. To investigate the nature of such changes, we measured Mg/Ca ratios in the planktonic foraminifera *G. bulloides* to produce a species-specific temperature record (Fig. 2f, g). This species is common from the subtropics to the SAF[20]. Accordingly, its abundance in TNO57-21 is relatively less sensitive to the abrupt frontal changes at our site, possibly because it is able to alter its growth habitat (for example by altering its growth season and or depth habitat) to minimize more rapid environmental fluctuations. As such, it is potentially a good candidate for monitoring more gradual changes in the background or ambient conditions.

The record of Mg/Ca ratios measured in *G. bulloides* (Fig. 2g) displays millennial-scale variability of a different nature from the polar fauna record. According to the Mg/Ca ratios, warming generally occurs during intervals of reduced polar species (that is, 'warm' intervals) and vice versa. This is similar to the relationship between the polar species record and Antarctic temperature records. The Mg/Ca record displays a similar deglacial pattern to the SST record from the southeast Pacific[13] (Fig. 2h), but in contrast with that record the highest Mg/Ca ratios (warmest temperatures) in TNO57-21 are observed during HS1. The highest measured Mg/Ca ratios within HS1 occur near the beginning and right at the end of the interval, with lower values occurring in between (Fig. 2g). This pattern is unexpected, given the continuous increase in warm-water species throughout the same interval. TNO57-21 was recovered from a deep-water (4,981-m) location and has probably experienced partial dissolution. Dissolution is known to affect planktonic foraminiferal Mg/Ca ratios in a systematic way, with increasing dissolution causing a progressive decrease in Mg/Ca (ref. 25). The record of foraminiferal fragmentation from TNO57-21 suggests that dissolution has varied through time at this site (Supplementary Information). Specifically, the interval of low Mg/Ca ratios during HS1 is precisely aligned with an interval of increased fragmentation. We infer from this that the Mg/Ca ratios are lower than expected as a direct result of dissolution.

To generate a reasonable estimation of temperature from the measured record of Mg/Ca ratios, we have employed a straightforward algorithm for adjusting the Mg/Ca record, based on an empirical calibration of Mg/Ca versus foraminiferal fragmentation (see Supplementary Information for a discussion of this approach). The procedure restores the warmer temperatures during HS1 (Fig. 2f). In fact, these temperatures may reasonably have been even higher, depending on the choice of calibration employed. Of particular importance is the overall preservation of structure within the Mg/Ca record. This provides confidence that we are not introducing significant artefacts into the record through adjustment of the data. Furthermore, the adjusted Mg/Ca ratios yield an early-Holocene temperature consistent with the location of TNO57-21 (the calibration used for converting Mg/Ca ratios to temperature is taken from ref. 26). Our Mg/Ca results suggest significant variations in temperature (Fig. 2f). The rise in temperature during the early part of HS1 is 4–5 °C (with or without adjustment of the data). The decrease in temperature during the Antarctic Cold Reversal is 2–3 °C using a three-point running mean or 4–5 °C without averaging.

We note that planktonic foraminiferal assemblages may also be sensitive to dissolution in that increased fragmentation will result in a proportional increase of more robust species (which tend to represent colder temperatures[27]). However, because we observe a decrease

in cold-water species (which are generally robust) and an increase in warm-water species (which are generally fragile) at the time of greatest fragmentation (Supplementary Information), we can be confident that these features are not an artefact of dissolution. In fact, the presence of warm-water species during HS1 may originally have been even greater than we observe.

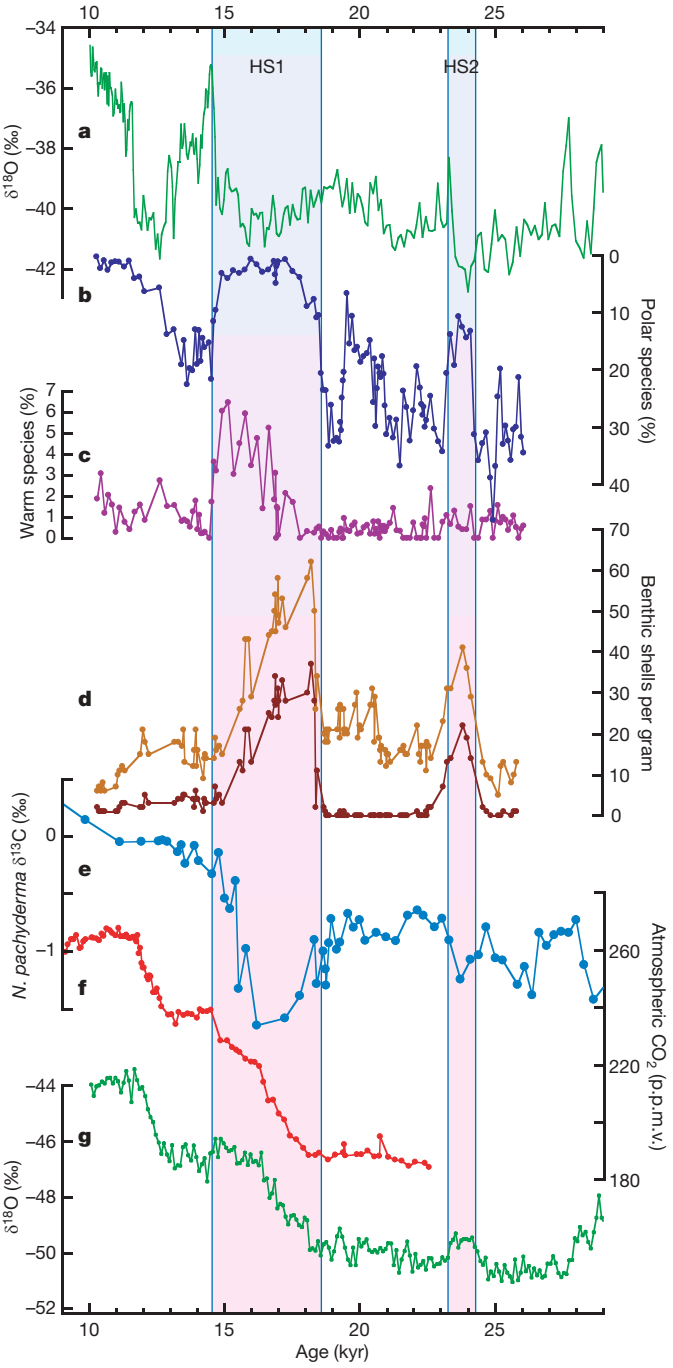

Figure 3 | Records of surface temperature and benthic fauna from TNO57-21. **a**, Greenland temperature (GISP2 ice core)[1]; **b**, polar foraminifera species in TNO57-21; **c**, warm foraminifera species; **d**, abundance of benthic foraminifera (upper curve) and *E. exigua* (lower curve); **e**, $\delta^{13}C$ in *N. pachyderma* from core RC11-83 (41.6° S, 9.8° E, 4,718 m)[17] ($\delta^{13}C = (^{13}C/^{12}C)_{sample}/(^{13}C/^{12}C)_{standard} - 1$; expressed relative to PeeDee Belemnite); **f**, atmospheric CO_2 (ref. 41; GICC05 timescale; see Supplementary Information); **g**, Antarctic temperature (EDML ice core)[5]. Shaded boxes represent Heinrich stadials and periods of Antarctic warming. Ice-core $\delta^{18}O$ values ($\delta^{18}O = (^{18}O/^{16}O)_{sample}/(^{18}O/^{16}O)_{standard} - 1$) are expressed relative to Vienna standard mean ocean water.

Surface ocean primary production

We also investigated changes in surface ocean productivity by analysing the benthic foraminiferal assemblages in TNO57-21 (Fig. 3d). The absolute abundance of benthic foraminifera shows two peaks (during HS1 and HS2). The magnitude of these peaks is driven largely by the presence of *Epistominella exigua*. In oligotrophic areas, this species is commonly associated with an increased flux of phytodetritus to the sea floor as a result of episodic phytoplankton blooms at the surface[28,29]. Today such events are commonly associated with the frontal systems of the Southern Ocean[30,31]. Along the STF, they occur as a direct consequence of turbulent eddy mixing across the front[31–33], which mixes nutrients from the sub-Antarctic zone into more stratified and warmer waters, thus creating suitable conditions for bloom development[34]. Increased surface production in the sub-Antarctic during the Heinrich events of Marine Isotope Stage (MIS) 3 has been reported previously[35], and it is significant that the episodes of increased *E. exigua* in TNO57-21 are associated only with the frontal movements inferred from the polar planktonic species during HS1 and HS2 and not with the shifts ~21 and ~26 kyr ago. This highlights the Heinrich stadials as unique within the deglacial sequence. We interpret the occurrence of *E. exigua* during HS1 and HS2 to reflect the proximity of the STF to TNO57-21 in combination with enhanced turbulence, possibly related to a strengthening of the ACC. This is supported by evidence from diatom assemblages in the same core (Supplementary Information). The sudden appearance of *E. exigua* at the beginning of HS1 is reminiscent of the abrupt change in polar species, and its more gradual decline coincides with the appearance of warm species and the increasing temperatures obtained from Mg/Ca ratios. Notably, a record of $\delta^{13}C$ in *N. pachyderma* (sinistral) from a nearby core[17] displays large negative values during the peaks of *E. exigua* abundance we observe in TNO57-21 (Fig. 3e). We suggest that these excursions reflect the advection of nutrient-rich waters across the STF during intervals of enhanced mixing along the front, supporting an increase in pulsed surface production.

Interhemispheric transmission

The characteristic responses of our proxy records may be placed in context by considering model simulations of abrupt changes in the AMOC (see, for example, refs 8–10, 36–38). Several mechanisms have been identified that might have an important role in the transmission of signals between the North Atlantic and the South Atlantic on timescales of decades[8–10,36] to several hundreds of years[9]. A persistent feature of the immediate (decadal) response to a slowdown in the AMOC is the southward shift of the intertropical convergence zone[8] and the westerly wind belts of the Southern Hemisphere[13,36]. A contemporaneous intensification of the ACC has also been reported as a direct consequence of increased westerly wind strength[10]. Our benthic fauna results suggest an increase in turbulent mixing across the northern fronts of the ACC during the AMOC slowdown of HS1, and therefore support the notion of an intensified ACC during this interval. Furthermore, the decline of polar foraminiferal species during Heinrich stadial events reflects the abrupt nature of southward shifts in the northern fronts of the ACC at these times. The 'instantaneous' bipolar mechanism is therefore not a straightforward temperature response, although some degree of rapid warming is predicted in the South Atlantic[8,9].

Our findings suggest that the ambient temperature response is more gradual, taking several hundreds of years. This reflects the build-up of heat within the South Atlantic as a consequence of a reduction in northward heat transport associated with a slowdown of the AMOC[6] combined with (during HS1) orbital forcing and possibly an increase in Agulhas leakage[21,37]. The propagation of thermal anomalies from the South Atlantic to Antarctica is slowed by the presence of the ACC[9], which represents a dynamical and thermal boundary between mid and high latitudes within the Southern Ocean[39] (note the delay between our ambient temperature increase

and Antarctic warming during HS1; Fig. 2f, i), although we would expect rapid transmission to other locations within the northern margin of the ACC (note the southeast Pacific record of ref. 13; Fig. 2f, h).

Our results appear to support a north-to-south transmission of abrupt changes across the Atlantic Ocean during deglaciation. However, they do not imply anything about the origin of such abrupt changes, which might be initiated by regional perturbations in the North Atlantic region (for example by freshwater forcing[8,10]) or as a nonlinear response to more gradual changes occurring remotely[40] (for example in the Southern Ocean)[37] or globally[38]. Furthermore, the Southern Ocean may provide a direct feedback on northern climate variability, for example through oceanic processes or atmospheric CO_2 (ref. 16).

CO_2 rise during Antarctic warming events

The close correspondence observed between atmospheric CO_2 and Antarctic temperature variability during the last deglaciation[41] (as well as during MIS 3[42]) indicates that the Southern Ocean has an important role in modulating atmospheric CO_2 on both glacial–interglacial and millennial timescales. Release of CO_2 during deglaciation may occur as a result of enhanced vertical mixing within the Southern Ocean[43,44], possibly as a result of a southerly shift in mid-latitude westerlies[43]. Intensification of the ACC during HS1, as suggested by our results and the modelling studies mentioned above, might have promoted the release of CO_2 by increasing the rate of vertical mixing within the Southern Ocean, thus contributing to the rise in atmospheric CO_2 at this time (Fig. 3f). This release of carbon may be reflected by the simultaneous 'leakage' of nutrients from within the Southern Ocean during HS1, as indicated by our benthic faunal records and the nearby record of planktonic $\delta^{13}C$ (ref. 17; Fig. 3). The more widespread occurrence of a planktonic $\delta^{13}C$ minimum event during the same interval[45] also supports this mechanism by the advection of nutrient- (and carbon-) rich waters away from the Southern Ocean, presumably by means of sub-Antarctic mode water formation[45].

The Heinrich stadials of MIS 3, and their corresponding Antarctic warming events, were also times of increasing atmospheric CO_2 (ref. 42), depleted planktonic $\delta^{13}C$ (ref. 17) and enhanced productivity in the sub-Antarctic region[35]. During the particularly prolonged interval of AMOC slowdown during HS1, the build-up of heat in the south and the release of CO_2 from the Southern Ocean (contributing to global warming in combination with, for example, insolation changes and ice-albedo feedbacks[46]) were apparently sufficient to enable deglaciation[15,38]. This mechanism may explain the rather abrupt onset of Antarctic temperature rise and the increase in atmospheric CO_2 at the start of deglaciation. We further speculate that during MIS 3 a similar mechanism was unable to drive deglaciation (possibly owing to orbital configuration[46] in combination with the subcritical size of continental ice sheets[47]), in which case the Antarctic warming events of MIS 3 may be thought of as 'failed terminations'.

METHODS SUMMARY

Sediment core samples were washed and sieved to 63 μm before drying and weighing. Planktonic foraminiferal faunal assemblage and fragment counts were performed on splits of the >150-μm fraction containing ~300 individual tests. Benthic foraminiferal counts were performed on the entire fraction >125 μm. Mg/Ca analyses were performed on typically 30 individual shells of *G. bulloides*, picked from the 250–315-μm fraction. Samples were prepared using the method of ref. 48 and analysed using a Finnigan Element XR high-resolution, inductively coupled plasma mass spectrometer. The age model for TNO57-21 was derived from 19 ^{14}C ages measured on *G. bulloides*. Two additional dates obtained from mixed species in a nearby core (RC11-83)[49] were used for the older part of the record. These were assigned depths on TNO57-21 by alignment of the records of percentage $CaCO_3$ from each core (Supplementary Fig. 1). ^{14}C ages were converted to calendar ages using a constant reservoir age of 600 yr.

Full Methods and any associated references are available in the online version of the paper at www.nature.com/nature.

Received 31 July 2008; accepted 12 January 2009.

1. Stuiver, M. & Grootes, P. M. GISP2 oxygen isotope ratios. *Quat. Res.* **53,** 277–283 (2000).
2. Bard, E., Rostek, F., Turon, J. L. & Gendreau, S. Hydrological impact of Heinrich events in the subtropical northeast Atlantic. *Science* **289,** 1321–1324 (2000).
3. Shackleton, N. J., Hall, M. A. & Vincent, E. Phase relationships between millennial-scale events 64,000-24,000 years ago. *Paleoceanography* **15,** 565–569 (2000).
4. Blunier, T. & Brook, E. J. Timing of millennial-scale climate change in Antarctica and Greenland during the last glacial period. *Science* **291,** 109–112 (2001).
5. EPICA Community Members. One-to-one coupling of glacial climate variability in Greenland and Antarctica. *Nature* **444,** 195–198 (2006).
6. Crowley, T. J. North Atlantic deep water cools the Southern Hemisphere. *Paleoceanography* **7,** 489–497 (1992).
7. Broecker, W. S. Paleocean circulation during the last deglaciation: A bipolar seesaw? *Paleoceanography* **13,** 119–121 (1998).
8. Vellinga, M. & Wood, R. A. Global climatic impacts of a collapse of the Atlantic thermohaline circulation. *Clim. Change* **54,** 251–267 (2002).
9. Schmittner, A., Saenko, O. A. & Weaver, A. J. Coupling of the hemispheres in observations and simulations of glacial climate change. *Quat. Sci. Rev.* **22,** 659–671 (2003).
10. Rind, D. *et al.* Effects of glacial meltwater in the GISS coupled atmosphere-ocean model - 2. A bipolar seesaw in Atlantic Deep Water production. *J. Geophys. Res.* **106,** 27355–27365 (2001).
11. Stocker, T. F. & Johnsen, S. J. A minimum thermodynamic model for the bipolar seesaw. *Paleoceanography* **18,** doi:10.1029/2003PA000920 (2003).
12. Wang, X. F. *et al.* Wet periods in northeastern Brazil over the past 210 kyr linked to distant climate anomalies. *Nature* **432,** 740–743 (2004).
13. Lamy, F. *et al.* Modulation of the bipolar seesaw in the southeast pacific during Termination 1. *Earth Planet. Sci. Lett.* **259,** 400–413 (2007).
14. McManus, J. F., Francois, R., Gherardi, J. M., Keigwin, L. D. & Brown-Leger, S. Collapse and rapid resumption of Atlantic meridional circulation linked to deglacial climate changes. *Nature* **428,** 834–837 (2004).
15. Denton, G. H., Broecker, W. S. & Alley, R. B. The mystery interval 17.5 to 14.5 kyrs ago. *PAGES News* **14,** 14–16 (2006).
16. Barker, S. & Knorr, G. Antarctic climate signature in the Greenland ice core record. *Proc. Natl Acad. Sci. USA* **104,** 17278–17282 (2007).
17. Ninnemann, U. S. & Charles, C. D. Regional differences in quaternary Subantarctic nutrient cycling: Link to intermediate and deep water ventilation. *Paleoceanography* **12,** 560–567 (1997).
18. Kanfoush, S. L. *et al.* Millennial-scale instability of the Antarctic ice sheet during the last glaciation. *Science* **288,** 1815–1818 (2000).
19. Johnsen, S. J., Dansgaard, W., Clausen, H. B. & Langway, C. C. Oxygen isotope profiles through Antarctic and Greenland ice sheets. *Nature* **235,** 429–434 (1972).
20. Niebler, H. S. & Gersonde, R. A planktic foraminiferal transfer function for the southern South Atlantic Ocean. *Mar. Micropaleontol.* **34,** 213–234 (1998).
21. Peeters, F. J. C. *et al.* Vigorous exchange between the Indian and Atlantic oceans at the end of the past five glacial periods. *Nature* **430,** 661–665 (2004).
22. Arz, H. W., Patzold, J. & Wefer, G. The deglacial history of the western tropical Atlantic as inferred from high resolution stable isotope records off northeastern Brazil. *Earth Planet. Sci. Lett.* **167,** 105–117 (1999).
23. Kim, J. H., Schneider, R. R., Muller, P. J. & Wefer, G. Interhemispheric comparison of deglacial sea-surface temperature patterns in Atlantic eastern boundary currents. *Earth Planet. Sci. Lett.* **194,** 383–393 (2002).
24. Farmer, E. C., deMenocal, P. B. & Marchitto, T. M. Holocene and deglacial ocean temperature variability in the Benguela upwelling region: Implications for low-latitude atmospheric circulation. *Paleoceanography* **20,** doi:10.1029/2004PA001049 (2005).
25. Barker, S., Cacho, I., Benway, H. & Tachikawa, K. Planktonic foraminiferal Mg/Ca as a proxy for past oceanic temperatures: a methodological overview and data compilation for the Last Glacial Maximum. *Quat. Sci. Rev.* **24,** 821–834 (2005).
26. Mashiotta, T. A., Lea, D. W. & Spero, H. J. Glacial-interglacial changes in Subantarctic sea surface temperature and $\delta^{18}O$-water using foraminiferal Mg. *Earth Planet. Sci. Lett.* **170,** 417–432 (1999).
27. Berger, W. H. Planktonic foraminifera: selective solution and the lysocline. *Mar. Geol.* **8,** 111–138 (1970).
28. Gooday, A. J. A response by benthic Foraminifera to the deposition of phytodetritus in the deep sea. *Nature* **332,** 70–73 (1988).
29. Cornelius, N. & Gooday, A. J. 'Live' (stained) deep-sea benthic foraminiferans in the western Weddell Sea: trends in abundance, diversity and taxonomic composition along a depth transect. *Deep-Sea Res. II* **51,** 1571–1602 (2004).
30. Froneman, P. W., Laubscher, R. K. & McQuaid, C. D. Size-fractionated primary production in the south Atlantic and Atlantic sectors of the Southern Ocean. *J. Plankton Res.* **23,** 611–622 (2001).
31. Saraceno, M., Provost, C. & Piola, A. R. On the relationship between satellite-retrieved surface temperature fronts and chlorophyll a in the western South Atlantic. *J. Geophys. Res.* **110,** doi:10.1029/2004JC002736 (2005).

32. Llido, J., Garcon, V., Lutjeharms, J. R. E. & Sudre, J. Event-scale blooms drive enhanced primary productivity at the Subtropical Convergence. *Geophys. Res. Lett.* **32,** doi:10.1029/2005GL022880 (2005).
33. Machu, E. *et al.* Phytoplankton distribution in the Agulhas system from a coupled physical-biological model. *Deep-Sea Res. I* **52,** 1300–1318 (2005).
34. Bathmann, U. V., Scharek, R., Klaas, C., Dubischar, C. D. & Smetacek, V. Spring development of phytoplankton biomass and composition in major water masses of the Atlantic sector of the Southern Ocean. *Deep-Sea Res. II* **44,** 51–67 (1997).
35. Sachs, J. P. & Anderson, R. F. Increased productivity in the subantarctic ocean during Heinrich events. *Nature* **434,** 1118–1121 (2005).
36. Timmermann, A., Krebs, U., Justino, F., Goosse, H. & Ivanochko, T. Mechanisms for millennial-scale global synchronization during the last glacial period. *Paleoceanography* **20,** doi:10.1029/2004PA001090 (2005).
37. Knorr, G. & Lohmann, G. Southern Ocean origin for the resumption of Atlantic thermohaline circulation during deglaciation. *Nature* **424,** 532–536 (2003).
38. Knorr, G. & Lohmann, G. Rapid transitions in the Atlantic thermohaline circulation triggered by global warming and meltwater during the last deglaciation. *Geochem. Geophys. Geosyst.* **8,** doi:10.1029/2007GC001604 (2007).
39. Cox, M. D. An idealized model of the world ocean. 1. The global-scale water masses. *J. Phys. Oceanogr.* **19,** 1730–1752 (1989).
40. Li, C., Battisti, D. S., Schrag, D. P. & Tziperman, E. Abrupt climate shifts in Greenland due to displacements of the sea ice edge. *Geophys. Res. Lett.* **32,** doi:10.1029/2005GL023492 (2005).
41. Monnin, E. *et al.* Atmospheric CO_2 concentrations over the last glacial termination. *Science* **291,** 112–114 (2001).
42. Ahn, J. & Brook, E. J. Atmospheric CO_2 and climate from 65 to 30 ka B.P. *Geophys. Res. Lett.* **34,** doi:10.1029/2007GL029551 (2007).
43. Toggweiler, J. R., Russell, J. L. & Carson, S. R. Midlatitude westerlies, atmospheric CO2, and climate change during the ice ages. *Paleoceanography* **21,** doi:10.1029/2005PA001154 (2006).
44. Kohler, P., Fischer, H., Munhoven, G. & Zeebe, R. E. Quantitative interpretation of atmospheric carbon records over the last glacial termination. *Glob. Biogeochem. Cycles* **19,** doi:10.1029/2004GB002345 (2005).
45. Spero, H. J. & Lea, D. W. The cause of carbon isotope minimum events on glacial terminations. *Science* **296,** 522–525 (2002).
46. Hays, J. D., Imbrie, J. & Shackleton, N. J. Variations in the Earth's orbit: Pacemaker of the ice ages. *Science* **194,** 1121–1132 (1976).
47. Raymo, M. E. The timing of major climate terminations. *Paleoceanography* **12,** 577–585 (1997).
48. Barker, S., Greaves, M. & Elderfield, H. A study of cleaning procedures used for foraminiferal Mg/Ca paleothermometry. *Geochem. Geophys. Geosyst.* **4,** doi:10.1029/2003GC000559 (2003).
49. Charles, C. D., Lynch-Stieglitz, J., Ninnemann, U. S. & Fairbanks, R. G. Climate connections between the hemispheres revealed by deep sea sediment core/ice core correlations. *Earth Planet. Sci. Lett.* **142,** 19–27 (1996).
50. Locarnini, R. A., Mishonov, A. V., Antonov, J. I., Boyer, T. P. & Garcia, H. E. *World Ocean Atlas 2005, Volume 1: Temperature* (ed. Levitus, S.) (NOAA Atlas NESDIS 61, US Govt Printing Office, 2006).

Supplementary Information is linked to the online version of the paper at www.nature.com/nature.

Acknowledgements We thank J. Riker and C. Lear for analytical advice and assistance and H. Medley for help with sediment processing. Sample material used in this project was provided by the Lamont-Doherty Earth Observatory Deep-Sea Sample Repository. We thank R. Lotti and G. Lozefski for help with sampling. Support for the collection and curating facilities of the core collection is provided by the US National Science Foundation through grant OCE00-02380 and the Office of Naval Research through grant N00014-02-1-0073. The work was supported by a National Science Foundation grant (OCE-0435703) to W.S.B. and S.B.

Author Contributions S.B. designed the research and performed foraminiferal Mg/Ca analyses, P.D. performed benthic foraminiferal counts and picked planktonic foraminifera for ^{14}C dating and Mg/Ca analyses, M.J.V. performed planktonic foraminiferal counts, J.P. performed diatom counts and G.K. helped with interpretation. All authors contributed towards preparing the manuscript.

Author Information Reprints and permissions information is available at www.nature.com/reprints. Correspondence and requests for materials should be addressed to S.B. (barkers3@cf.ac.uk).

METHODS

Age control. Age control for TNO57-21 was determined from a combination of 19 monospecific ^{14}C dates on *G. bulloides* (measured at the National Ocean Sciences Accelerator Mass Spectrometry Facility) and additional ^{14}C ages from a nearby core (RC11-83)[49]. The two cores were spliced together by means of their records of percentage $CaCO_3$, which contain sufficient structure to allow robust tuning with an estimated error $<\pm 10$ cm or $\sim$600 yr (Supplementary Fig. 1). To attain sufficient sample weight for ^{14}C dating, tests of *G. bulloides* were combined from five consecutive 1-cm intervals of core. Therefore, each ^{14}C age represents a 5-cm interval ($\sim$300 yr of sedimentation). Tests of *G. bulloides* were picked from the 250–315-μm fraction or $>$250 μm where sample size was small. ^{14}C ages were converted to calendar ages using CALIB[51] software (version 5.0.1) with the Marine04 calibration curve[52] and $\Delta R = 200$ yr (that is, reservoir age of 600 yr). For samples older than 24 kyr (^{14}C) the calibration software of ref. 53 was employed (Supplementary Table 1). A surface reservoir correction of 600 yr was chosen to account for the relatively high southerly latitude of the core site and the possibility that glacial reservoir ages may have been slightly higher than modern in this region[54]. The age control points for RC11-83 given in Supplementary Table 1 were used to recalculate the age model for the $\delta^{13}C$ record of *N. pachyderma* (sinistral)[17] shown in Fig. 3 of the main text.

Faunal assemblage counts. Planktonic foraminiferal counts were performed on 1-cm intervals of sediment with a sampling frequency of 2 cm, following the taxonomy of ref. 55. Each sample was split to provide $>$300 individuals in the $>$150-μm fraction (only two samples contained fewer than 100 individuals). Planktonic foraminiferal fragment counts were made at the same time on the same sample splits. The abundance of benthic foraminifera was generally low ($\sim$100 individuals on average); therefore, all individuals from the $>$125-μm fraction were counted. Sampling frequency was every 1 to 5 cm for the benthic counts.

Mg/Ca ratios in *G. bulloides*. Mg/Ca ratios in *G. bulloides* were measured every 2 cm. Tests of *G. bulloides* were picked from the 250–315-μm fraction and prepared for analysis following the procedure of ref. 48, with an additional centrifuge step after dissolution. Typically 30 tests were used per sample; fewer where samples were small. Analyses were performed on a Finnigan Element XR (extended dynamic range) inductively coupled plasma mass spectrometer. Typical within-run precision was $0.35 \pm 0.2\%$, with long-term precision $<2\%$. Simultaneous determination of Fe and Al allowed for the assessment of silicate contamination. One sample from a total of 124 was rejected on the basis of its Fe/Mg ratio[48] (Supplementary Fig. 2).

Atmospheric CO_2. The record of atmospheric CO_2 from ref. 41 was placed on the GICC05 timescale[56] (as used for the EDML $\delta^{18}O$ record[5]) by shifting the latest EDC3[57] timescale by 500 yr to align the records of CH_4 (Supplementary Fig. 9).

51. Stuiver, M. & Reimer, P. J. Extended ^{14}C data-base and revised Calib 3.0 ^{14}C age calibration program. *Radiocarbon* **35,** 215–230 (1993).
52. Hughen, K. A. *et al.* Marine04 marine radiocarbon age calibration, 0-26 cal kyr BP. *Radiocarbon* **46,** 1059–1086 (2004).
53. Fairbanks, R. G. *et al.* Radiocarbon calibration curve spanning 0 to 50,000 years BP based on paired Th-230/U-234/U-238 and C-14 dates on pristine corals. *Quat. Sci. Rev.* **24,** 1781–1796 (2005).
54. Bard, E. Correction of accelerator mass spectrometry ^{14}C ages measured in planktonic foraminifera: paleoceanographic implications. *Paleoceanography* **3,** 635–645 (1988).
55. Kennett, J. P. & Srinivasan, M. S. *Neogene Planktonic Foraminifera: A Phylogenetic Atlas* (Wiley, 1983).
56. Andersen, K. K. *et al.* A 60 000 year Greenland stratigraphic ice core chronology. *Clim. Past Discuss.* **3,** 1235–1260 (2007).
57. Parrenin, F. *et al.* The EDC3 chronology for the EPICA dome C ice core. *Clim. Past* **3,** 485–497 (2007).